Fundamental Journals
International Journal of Fundamental Physical Sciences (IJFPS) ISSN:2231-8186
IJFPS, Vol 4, No 4, pp 105-110, Dec , 2014 ***M. E. Emetere***
DOI:10.14331/ijfps.2014.330073
http://dx.doi.org/10.14331/ijfps.2014.330073

Femtosecond Spin Dynamics Mechanism In Graphenes: The Bloch NMR-Schrödinger Probe

Moses E. Emetere [1]*, Bijan Nikouravan [2]

[1]Department of Physics, Covenant University Canaan land, P.M.B 1023, Ota, Nigeria
E-mail: moses.emetere@covenantuniversity.edu.ng
[2]Department of Physics, Faculty of Science, Islamic Azad University (IAU), Varamin, Iran
E-mail: nikou@iauvaramin.ac.ir

(*Received March 2014; Published Dec 2014*)

ABSTRACT

The mechanism of the femtosecond spin dynamics is still not properly understood. The remodeled Bloch-Schrödinger equation was incorporated into the Hamiltonian. The mechanism of the femtosecond dynamics was investigated under three quantum states. The spin relaxation mechanism operated in a single continuous time scale (>70ps) which was in variance with known postulate. The transient reflectivity was measured to be within an angular range of 18.6^o to 90.0^o at a pulse range of 1MHz to 6.5 MHz. Beyond the pulse intensity of -2.5, the system elapsed into a quasi-equilibrium state which explains the independence of the magnetic moment on the pulse intensity. Different possibilities of the femtosecond spin dynamics were worked out for future study.

Keywords: femtosecond spin dynamics, Schrödinger, Bloch NMR, spin relaxation

DOI:10.14331/ijfps.2014.330073

INTRODUCTION

Justifying novel experimental research by theoretical models is fast deviating from the usual practice of merely combining theories and mathematical conditions into a robust process of setting pace for experimental research by proactive theoretical models. The femtosecond spin dynamics of materials is a typical research area which has shown as much complexities as the superconducting medium. For example, the graphene was reported to be in the class of an ideal spintronics (Fabian, Matos-Abiague, Ertler, Stano, & Žutić, 2007). Its spin relaxation mechanism still remains uncertain due to wide discrepancies between experimental (Jo, Ki, Jeong, Lee, & Kettemann, 2011; Tombros et al., 2008) (Kotov, Uchoa, Pereira, Guinea, & Neto, 2012) and theoretical efforts (Dugaev, Sherman, & Barnaś, 2011; Han et al., 2012; Ochoa, Neto, & Guinea, 2012; Zhou & Wu, 2010). The spin relaxation in graphene and spintronics had been reported to dependent on adatoms (Yazyev, 2010), curvature (Jeong, Shin, & Lee, 2011), substrate effects (Dedkov, Fonin, Rüdiger, & Laubschat, 2008; Emetere, 2013a) , vacancies (Nair et al., 2012) and contacts (Popinciuc et al., 2009). Often times, there had been scientific reports of strange twist of behavioral and functionality of materials at certain conditions. For example, at the same time scale i.e. 100ps, spin relaxation time in graphene is due to resonant scattering by local magnetic moments (Kochan, Gmitra, & Fabian, 2014); in GD, spin-lattice interaction is dominant (Vaterlaus, Beutler, & Meier, 1991); in nickel, a sharp decrease of magnetization was observed (Hohlfeld, Matthias, Knorren, & Bennemann, 1997; Hübner & Zhang, 1998). These discoveries show that theoretical research may be unable to discover the mechanism of different material due to dissimilar reactions to physical conditions (Emetere, Uno, & Isah, 2014). Recent experiment on mesoscopic transport (Lundeberg, Yang, Renard, & Folk, 2013) showed the importance of the local magnetic moment in spin relaxation. Fortunately, the phenomenon of magnetic resonance is hinged on the interplay between magnetic moments and angular momentum. The importance of the nuclear magnetic resonance (NMR) to observe the transitions in different spin states (due to the breaking of the energy degeneracy by

magnetic field) cannot be overestimated (Emetere, 2013a, 2013d, 2014a, 2014b; Melissinos & Napolitano, 2003; U. Uno & Emetere, 2012). The NMR works on the interaction of the nuclear spin system which in their original form are quantum state. Theoretically, some quantum state referred to in the later part of this paper e.g quasi-equilibrium state does not evolve under Hamiltonian system except they are reduced with the eigenbasis blocks of the spin environment Hamiltonian (Walls & Lin, 2006).

This problem was solved in this paper by estimating-differently for the reduction of the eigenbasis blocks of the spin environment Hamiltonian-using the Bloch NMR equation to solve the Schrödinger equations (Emetere, 2013b, 2014c) and then inserting the solutions (which are the reduced eigenbasis) into a spin environment Hamiltonian in order to analyze the mechanism of femtosecond spin dynamics. Recall that validity of the NMR relaxation rates to analyze the femtosecond spin dynamics had been confirmed in the experimental investigation on the molecular rotation and intermolecular motions from picosecond to nanosecond time scale (Ishima & Torchia, 2000; Palmer III, 2001).

THEORETICAL BACKGROUND

The generic Hamiltonian proposed is shown below

$$H_T = H_n + H_s(t) \tag{1}$$

Here H_n is the time independent Hamiltonian which is written as

$$H_n = H_u + H_v \tag{2}$$

and H_u is the electron Zeeman interaction which accounts for the coulomb repulsion, exchange interaction and exchange anisotropy of the electron interaction. For the purpose of this research the Zeeman electron interaction is discussed as a single integrated unit-with respect to the magnetic field. H_v is the nuclear Zeeman interaction. The Zeeman electron interaction ranges within a frequency of 1-10GHz while the Zeeman nuclear interaction ranges within a frequency of 1-10MHz. Since the Zeeman interaction is the interaction between spin and magnetic field, we introduced the solution of the solved Bloch NMR-Schrödinger (Emetere, 2013b, 2013c; Emetere et al., 2014) as the initial Hamiltonian for the nuclear Zeeman interaction i.e.

$$H = 1 - m.\omega_1 M_y T_1 \tag{3}$$

Where $\omega_1 = -\gamma B_1$ the Rabi frequency, m is is the magnetic moment, M_y is the applied transverse magnetization and T_1 is the spin-lattice relation time. The total magnetic field at the nuclei is different to the applied magnetic field (M_y). Therefore, the total magnetic field (M_T) at the nuclei is given as

$$M_T = (1 - \sigma)M_y \tag{4}$$

Where σ is referred to as a second ranked tensor which relates the applied magnetic field (M_y) and the total magnetic field (M_T). The final formulation of the Hamiltonian is realized by incorporating Eq (4) into Eq(3) as

$$H_v = \frac{M_T}{M_y} + \sigma - m.\omega_1 M_y T_1 \tag{5}$$

The Zeeman electron interaction Hamiltonian is defined as shown below

$$H_u = m\hbar\gamma M_y \tag{6}$$

Where $\hbar$ is the Planck's constant and γ is the gyromagnetic ratio. The combined Hamiltonian is given as

$$H_n = \frac{M_T}{M_y} + \sigma - m.M_y(\omega_1 T_1 + \hbar\gamma) \tag{7}$$

The dominance of the transverse magnetization gave rise to an assumption that the term ($H_s(t)$) as shown in Eq(1) is a vanishing spin-lattice coupling term. The system state in the Hamiltonian is critical because it is fully described by the spin-density matrix. Therefore, we relate the spin-density matrix to the vital components of the general Hamiltonian (H_n). To proof that $H_s(t)$ is a vanishing spin-lattice coupling term, we apply R(t) to all operators R in the laboratory frame

$$R \to \bar{R}(t) = \exp\big(iH(t)\big)\, R \exp\,(-iH(t)) \tag{8}$$

Differentiating (8)

$$\frac{d\bar{R}(t)}{dt} = \frac{d}{dt}\big[\exp\big(iH(t)\big)\, R \exp\,(-iH(t))\big] \tag{9}$$

$$\frac{d\bar{R}(t)}{dt} = iH(t)R + \exp\big(iH(t)\big)\frac{dR}{dt}\exp\big(-iH(t)\big) - iRH(t) \tag{10}$$

Where $\frac{dR}{dt}$ is defined by the Liouville-Von Neuman as

$$\frac{dR}{dt} = -i[H_T, R]$$

$$\frac{d\bar{R}(t)}{dt} = i[H(t), R] - i\exp\big(iH(t)\big)\,[H_n + H_s(t), R]\exp\big(-iH(t)\big) \tag{11}$$

To solve for the last term of the right hand side, we adopt the rule

$$U(X,Y)U^{\dagger} = [UXU^{\dagger}, UYU^{\dagger}] \tag{12}$$

Let $U = \exp\,(iH(t)$ and $U^{\dagger} = \exp\,(-iH(t))$. The product of the two terms ($UU^{\dagger} = 1$) shows that the terms are Hermitian conjugate unitary operator. Equation 11 transforms to

$$\frac{d\bar{R}(t)}{dt} = i[H(t), R] - i[H_n + H_s(t), R] \tag{13}$$

Equation 13 reduced to

$$\frac{d\bar{R}(t)}{dt} = -i[H_n, R] \tag{14}$$

By the characteristics of Eq(14), R refers to the spin density matrix, H_n is a dynamic Hamiltonian which we have derived in Eq(7). To solve the spin density matrix relating to

the time t, Eq(14) is integrated within the boundaries of 0 and t.

$$R(t) = -i\int_0^t [H_n, R]dt + R(0) \quad (15)$$

If the time factor for interaction within the electron and nucleus is accounted for in Eq(15), it becomes

$$R(t) = R(0) - i\int_0^t [H_n, R(t)]dt \quad (16)$$

The effect of time factor in H_n is in the transformation of the second ranked tensor (which represents the chemical shift). At this point, the resonance frequency is unstable with respect to the spins. R(t) therefore decays (Goldman, 2001) to

$$R(t) = \exp(i\omega_\alpha t)\, R \quad (17)$$

Now, we mathematically accounted for the reduction of the eigenbasis blocks of the spin environment Hamiltonian-using the Bloch NMR equation to solve the Schrödinger equations and then inserting the solutions (which are the reduced eigenbasis) into a spin environment Hamiltonian in order to analyze the mechanism of femtosecond spin dynamics in the next section.

RESULTS AND DISCUSSION

The initial assumption made in this paper is that the nucleus and the electrons are enclosed in a spherical boundary called atom. We applied the Christoffel's second rank tensor analysis within a spherical polar coordinate,

$$(ds)^2 = (dr)^2 + r^2(d\theta)^2 + r^2 sin^2(\theta)(d\emptyset)^2 \quad (18)$$

The many solutions can be found in Gupta (2010) as

$$\sigma = sin\theta cos\theta \quad , \quad \sigma = cot\theta \quad , \quad \sigma = -rsin^2\theta \quad (19c)$$

The solutions in Eq(19) are important to characterize the spin relaxations under three conditions (low transverse magnetization, moderate transverse magnetization and high transverse magnetization) at 100ps time scale. This idea would avail us the validity to affirm the presence of magnetic deflagration in the graphene sample (see Fig (1) to Fig (3)).

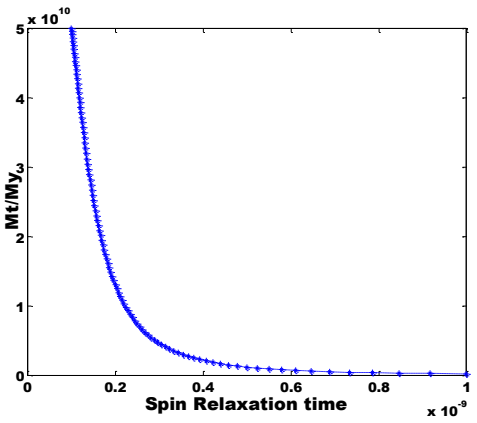

Fig 1. Spin relaxation at low transverse magnetization

Magnetic deflagration has been earlier reported as the signature of magnetic material prepared in a metastable spin configuration (Subedi et al., 2013).

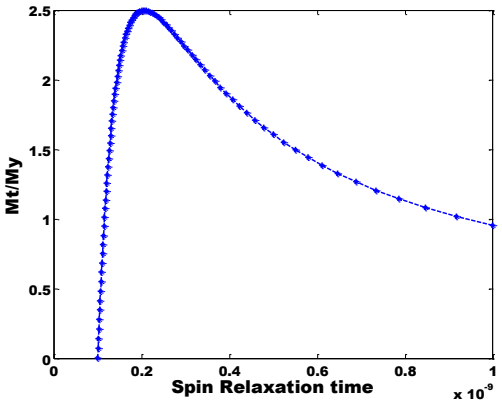

Fig 2. Spin relaxation at moderate transverse magnetisation.

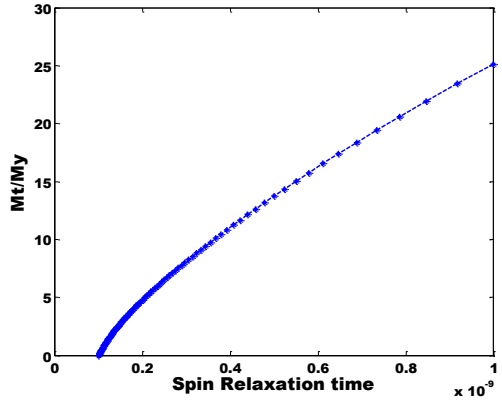

Fig3. Spin relaxation at high transverse magnetization

Experimentally, the time needed to reverse spins is given as about 100ps (Zhang & Hübner, 1999). Also, the characteristic time for establishing a thermal equilibrium between the lattice and the spin system is also within the range of 100ps (Vaterlaus et al., 1991). We restricted the research within the 0ps-100ps because the spin lattice interaction for some materials (Beaurepaire, Merle, Daunois, & Bigot, 1996; Hohlfeld et al., 1997) seem to be more visible at this range. One of the significant successes of the Bloch –Schrodinger solutions was the splitting of overlapping resonances without the usual long measuring times as shown in Fig(1-3). Also, the Bloch-Schrodinger solutions could be used to analyze coupled spin systems unlike the restriction to the uncoupled spin which the Bloch NMR equation is known for. When the applied transverse magnetization is very low, the features in Fig(1) reveals the following occurrences: the magnetic ratio (M_T/M_y) curve defines the nature of demagnetization on the femtoscale as electronic (Hohlfeld et al., 1997); two-spin correlations dominates the coherent dynamics during the early timescale (Hübner & Zhang, 1998); the transition from ferromagnetism to paramagnetism is not restricted only to heating the system temperature above the Curie point.

Changing the pulse sequencing of the applied transverse magnetization could also initiate the transition from ferromagnetism to paramagnetism (Uno E . Emetere 2011). The experimental effect of pulse sequencing of the applied transverse magnetization e.g. competing relaxation pathways was accounted for in this calculations.

At about 40ps (as shown in Fig (1)), the spin system recognized the impact of the total effect of the magnetic field on the material nuclei. This can be practically summarized that low applied transverse magnetization favors the analysis of Gd whose spin-lattice relaxation time was experimental reported as 48ps (Schneider et al., 2006). When the transverse magnetization is increased (as shown in Fig (2)), coherence was preserved though the spin relaxation time increased to 60ps which favors the analysis of GaAs (100) and doped graphene (Popinciuc et al., 2009; Scholl, Baumgarten, Jacquemin, & Eberhardt, 1997; U. E. Uno, Emetere, Isah, & Ahmadu, 2012; WILLIAMS, 2014); Uno et al., 2014). At high applied transverse magnetization, coherence was still preserved (as shown in Fig (3)) though the spin relaxation time increased to 70ps which favors the analysis of GaAs (011) (Chan et al., 2012). Beyond the fundamental explanation of Fig (3), the ultrafast demagnetization surfaced. As against the idea of (Scholl et al., 1997) which predicted two time-scale for spin relaxation mechanism, Fig (3) showed a single continuous time scale (>70ps). Further explanation is drawn from Fig (4) where the angular changed of the chemical shift was investigated under varying frequencies within the range of 1MHz -10MHz as specified earlier in the Zeeman nuclear interaction range. The angular change of the chemical shift which affects the structural changes of the compound (whose idea was developed from the experimental set-up in Chan et al. (2012) was incorporated to properly analyze the effect of the nonmagnetic artifacts (Bigot, Guidoni, Beaurepaire, & Saeta, 2004; Carva, Battiato, & Oppeneer, 2011; Emetere & Bakeko, 2013; U. E. Uno et al., 2012) which could alter the magnetic asymmetry via the transient change of the refractive index (Chan et al., 2012). The overlapping signals was resolved spectroscopically by transient-reflectivity adjustments via the parameter assumed for the angular change and the incorporation of the Bohr's radius for the value of ' r ' as shown in Eq(19). Within the 0 to π pulses, a Gaussian shape emerged between the demagnetization and the angular changes in the chemical shift which indicates a laminar shift in the selective pulses. Also, the Gaussian shape occurred between the demagnetization and the pulse which was measured to be between 1MHz to 6.5 MHz. The transient reflectivity was also measured to be within range of 18.6^{o} and 90^{o}. Beyond the 6.5 MHz, the demagnetization showed no significant changes. This showed that the material has transited into the dichroic bleaching state where the electrons are in a non-equilibrium state. At the same pulse range, another state was discovered in Fig(5). The material transient to an equilibrium state where the electrons are said to be in equilibrium as shown by the parallel shape on the demagnetization-pulse axes in Fig(5). In this state, the spin flip increases the number of electrons with opposite sign as shown by the parabolic shape on the demagnetization-angular chemical shift axes. This occurrence is one of the factors responsible for the absence of signal in the copper wire used in an experiment conducted by (Shikoh et al., 2013). When the spin flip (which is associated to the spin orbit coupling in a quantum well) recovers i.e eliminating the electrons with opposite signs, the inverse spin hall effect (ISHE) is forced into a quasi-equilibrium which resist the flow of signal through the copper wire. This assertion can be observed in the parallel platform in Fig(5). Experimentally, the parallel platform can be raised by doping the material.

In Fig(6) we tested the explicit dependence of the magnetic moment on pulse intensity. The result was in agreement with the postulate of (Zhang & Hübner, 1999) i.e spin orbital coupling alone is not sufficient to yield a clear reduction of the magnetic moment (as discussed above). The demagnetization was also true that it was roughly proportional to the spin orbit coupling constant. Notably, the (Zhang & Hübner, 1999) was negative curve, Fig(6) is a positive curve which explains why the change of magnetization is moderate for materials like graphene despite the bleaching effect whose saturation for intensity was calculated as $I \leq -2.5$. Beyond the intensity $I > -2.5$, there is no effect on the magnetic moment because it is at its quasi-equilibrium state.

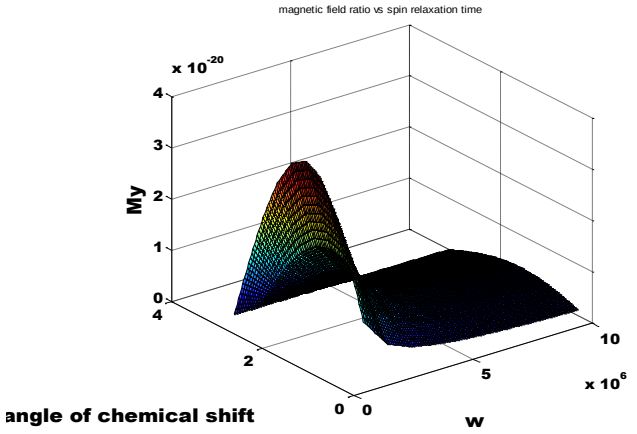

Fig4. Effect of transverse magnetization on the angular changes of the chemical shift.

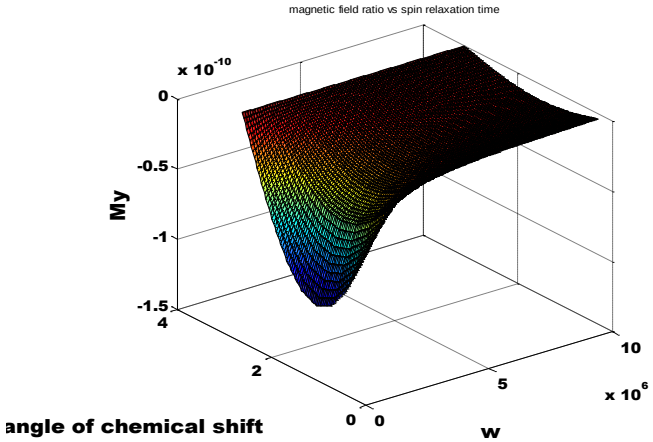

Fig 5. Effect of transverse magnetization on the angular changes of the chemical shift in a stable state

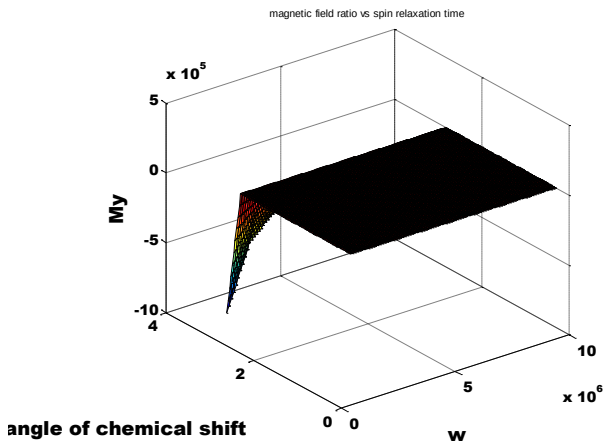

Fig6. Effect of intensity dependence on the magnetic moment

CONCLUSION

In conclusion, three states were discovered in the femtosecond spin dynamics mechanism. The first is the blocking state where the electrons are in a non-equilibrium state. The measurement at this state specifies that its transient reflectivity is within an angular range of 18.6^{o} to 90.0^{o}. The pulse was within the range of 1MHz to 6.5 MHz. The second was the equilibrium state where the spin flip increases the number of electrons with opposite sign. The third is the quasi-equilibrium state where the pulse intensity had moderate impact on the magnetic moment under the bleaching effects when $I \leq -2.5$. Beyond the intensity $I > -2.5$, there is no effect on the magnetic moment because it is at its quasi-equilibrium state. In variance with the idea of (Scholl et al., 1997) who proposed two time scales, the research showed a single continuous time scale (>70ps). This may be due to the Bauschinger effect present in heterogeneous compounds (Emetere, 2014a).

ACKNOWLEDGEMENT

The authors acknowledge the supports of their host institutions and J. Emetere.

REFERENCES

Beaurepaire, E., Merle, J.-C., Daunois, A., & Bigot, J.-Y. (1996). Ultrafast spin dynamics in ferromagnetic nickel. *Physical review letters*, *76*(22), 4250.

Bigot, J.-Y., Guidoni, L., Beaurepaire, E., & Saeta, P. N. (2004). Femtosecond spectrotemporal magneto-optics. *Physical review letters*, *93*(7), 077401.

Carva, K., Battiato, M., & Oppeneer, P. M. (2011). Is the controversy over femtosecond magneto-optics really solved? *Nature Physics*, *7*(9), 665-665.

Chan, L.-O., Turgut, E., Teale, C. A., Kapteyn, H. C., Murnane, M. M., Mathias, S., Nembach, H. T. (2012). Ultrafast demagnetization measurements using extreme ultraviolet light: comparison of electronic and magnetic contributions. *Physical Review X*, *2*(1), 011005.

Dedkov, Y. S., Fonin, M., Rüdiger, U., & Laubschat, C. (2008). Rashba effect in the graphene/Ni (111) system. *Physical review letters*, *100*(10), 107602.

Dugaev, V., Sherman, E. Y., & Barnaś, J. (2011). Spin dephasing and pumping in graphene due to random spin-orbit interaction. *Physical Review B*, *83*(8), 085306.

Emetere, M. E. (2013a). Mathematical Modelling of Bloch NMR to Explain the Rashba Energy Features. *World Journal of Condensed Matter Physics*, *3*, 87.

Emetere, M. E. (2013b). MATHEMATICAL MODELLING OF BLOCH NMR TO SOLVE THE SCHRODINGER TIME DEPENDENT EQUATION. *The African Review of Physics*, *8*.

Emetere, M. E. (2013c). Modeling the Non-Single Exponential Photoluminescence Decay Using the Boubaker Polynomial Expansion Scheme. *Journal of Advanced Physics*, *2*(3), 213-215.

Emetere, M. E. (2013d). Quantum Information Technology Based on Magnetic Excitation of Single Spin Dynamics. *Industrial Engineering Letters*, *3*(5), 33-36.

Emetere, M. E. (2014a). Characteristic Significance Of Magnetic Relaxations On Copper Oxide Thin Film Using The Bloch Nmr. *Surface Review and Letters*, *21*(05).

Emetere, M. E. (2014b). Mathematical Modelling of Bloch NMR to Solve the Schrödinger Time Dependent Equation. *Applied Mathematical Sciences*, *8*(56), 2753 – 2762.

Emetere, M. E. (2014c). Profiling Laser-Induced Temperature Fields for Superconducting Materials Using Mathematical Experimentation. *Journal of Thermophysics and Heat Transfer*, *28*(4), 700-707.

Emetere, M. E., & Bakeko, M. M. (2013). Determination of characteristic relaxation times and their significance in copper oxide thin film. *Journal of the theoretical Physics and Cryptography*, *4*(1), 1-4.

Emetere, M. E., Uno, U. E., & Isah, K. (2014). A Remodeled Stretched Exponential–Decay Formula for Complex Systems. *RESEARCH & REVIEWS: JOURNAL OF ENGINEERING AND TECHNOLOGY*, *3*(2), 4-12.

Fabian, J., Matos-Abiague, A., Ertler, C., Stano, P., & Žutić, I. (2007). Semiconductor spintronics. *Acta Physica Slovaca. Reviews and Tutorials*, *57*(4-5), 565-907.

Han, W., McCreary, K., Pi, K., Wang, W., Li, Y., Wen, H., . Kawakami, R. (2012). Spin transport and relaxation in graphene. *Journal of Magnetism and Magnetic Materials*, *324*(4), 369-381.

Hohlfeld, J., Matthias, E., Knorren, R., & Bennemann, K. (1997). Nonequilibrium magnetization dynamics of nickel. *Physical review letters*, *78*(25), 4861.

Hübner, W., & Zhang, G. (1998). Femtosecond spin dynamics probed by linear and nonlinear magneto-optics. *Journal of Magnetism and Magnetic Materials*, *189*(1), 101-105.

Ishima, R., & Torchia, D. A. (2000). Protein dynamics from NMR. *Nature Structural & Molecular Biology*, *7*(9), 740-743.

Jeong, J.-S., Shin, J., & Lee, H.-W. (2011). Curvature-induced spin-orbit coupling and spin relaxation in a chemically clean single-layer graphene. *Physical Review B, 84*(19), 195457.

Jo, S., Ki, D.-K., Jeong, D., Lee, H.-J., & Kettemann, S. (2011). Spin relaxation properties in graphene due to its linear dispersion. *Physical Review B, 84*(7), 075453.

Kochan, D., Gmitra, M., & Fabian, J. (2014). Spin relaxation mechanism in graphene: resonant scattering by magnetic impurities. *Physical review letters, 112*(11), 116602.

Kotov, V. N., Uchoa, B., Pereira, V. M., Guinea, F., & Neto, A. C. (2012). Electron-electron interactions in graphene: Current status and perspectives. *Reviews of Modern Physics, 84*(3), 1067.

Lundeberg, M. B., Yang, R., Renard, J., & Folk, J. A. (2013). Defect-mediated spin relaxation and dephasing in graphene. *Physical review letters, 110*(15), 156601.

Melissinos, A. C., & Napolitano, J. (2003). *Experiments in modern physics*: Gulf Professional Publishing.

Nair, R., Sepioni, M., Tsai, I.-L., Lehtinen, O., Keinonen, J., Krasheninnikov, A., . . . Grigorieva, I. (2012). Spin-half paramagnetism in graphene induced by point defects. *Nature Physics, 8*(3), 199-202.

Ochoa, H., Neto, A. C., & Guinea, F. (2012). Elliot-yafet mechanism in graphene. *Physical review letters, 108*(20), 206808.

Palmer III, A. G. (2001). NMR probes of molecular dynamics: overview and comparison with other techniques. *Annual review of biophysics and biomolecular structure, 30*(1), 129-155.

Popinciuc, M., Józsa, C., Zomer, P., Tombros, N., Veligura, A., Jonkman, H., & Van Wees, B. (2009). Electronic spin transport in graphene field-effect transistors. *Physical Review B, 80*(21), 214427.

Schneider, H., Wüstenberg, J.-P., Andreyev, O., Hiebbner, K., Guo, L., Lange, J., . . . Aeschlimann, M. (2006). Energy-resolved electron spin dynamics at surfaces of p-doped GaAs. *Physical Review B, 73*(8), 081302.

Scholl, A., Baumgarten, L., Jacquemin, R., & Eberhardt, W. (1997). Ultrafast spin dynamics of ferromagnetic thin films observed by fs spin-resolved two-photon photoemission. *Physical review letters, 79*(25), 5146.

Shikoh, E., Ando, K., Kubo, K., Saitoh, E., Shinjo, T., & Shiraishi, M. (2013). Spin-pump-induced spin transport in p-Type Si at room temperature. *Physical review letters, 110*(12), 127201.

Subedi, P., Vélez, S., Macià, F., Li, S., Sarachik, M., Tejada, J., . . . Kent, A. (2013). Onset of a propagating self-sustained spin reversal front in a magnetic system. *Physical review letters, 110*(20), 207203.

Tombros, N., Tanabe, S., Veligura, A., Jozsa, C., Popinciuc, M., Jonkman, H., & Van Wees, B. (2008). Anisotropic spin relaxation in graphene. *Physical review letters, 101*(4), 046601.

Uno E . Emetere (2011). Mean-Field Analysis Of The Layering Transitions Of The Spin- 1/2 Ising Model In A Transverse Magnetic Field. *Int. Journal for scientific research, 1*(1), 7-13.

Uno, U., & Emetere, M. E. (2012). Analysis of the High Temperature Superconducting Magnetic Penetration Depth Using the Bloch NMR Equations. *Global Engineers and Technologist Review, 2*(1), 14-21.

Uno, U. E., Emetere, M. E., Isah, K., & Ahmadu, U. (2012). On The Effect of Electron-Hole Recombination in Disordered GaAs-Aa1-xALAs Multi-quantum Well Structure. *International Journal of Fundamental Physical Sciences, 2*(4).

Vaterlaus, A., Beutler, T., & Meier, F. (1991). Spin-lattice relaxation time of ferromagnetic gadolinium determined with time-resolved spin-polarized photoemission. *Physical review letters, 67*(23), 3314.

Walls, J. D., & Lin, Y.-Y. (2006). Constants of motion in NMR spectroscopy. *Solid state nuclear magnetic resonance, 29*(1), 22-29.

WILLIAMS, O. (2014). EVIDENCE OF POSITIONAL DOPING EFFECTS ON THE OPTICAL PROPERTIES OF DOPED TIN DIOXIDE (SnO2) WITH ZINC (Zn). *Journal of Ovonic Research Vol, 10*(4), 141-147.

Yazyev, O. V. (2010). Emergence of magnetism in graphene materials and nanostructures. *Reports on Progress in Physics, 73*(5), 056501.

Zhang, G., & Hübner, W. (1999). Femtosecond spin dynamics in the time domain. *Journal of applied physics, 85*(8), 5657-5659.

Zhou, Y., & Wu, M. (2010). Electron spin relaxation in graphene from a microscopic approach: Role of electron-electron interaction. *Physical Review B, 82*(8), 085304.

